Article

J. Mex. Chem. Soc. **2007**, *51(2),* 47-54

ISSN 1870-249X

Decomposition and Cyanidation Kinetics of the Argentian Ammonium Jarosite in NaOH Media

Antonio Roca,[1] Francisco Patiño,*[2] Isauro Rivera,[2] Leticia Hernández,[2] Miguel Pérez,[2] Eleazar Salinas[2] and Martín Reyes[2]

[1] Departamento d´ Enginyeria Química i Metal.lúrgia, Universitat de Barcelona. Martí i Franquès 1, 08028, Barcelona, España. Tel.(34) 93 – 4021295. e-mail: roca@material.qui.ub.es

[2] Centro de Investigaciones en Metalurgia y Materiales, Universidad Autónoma del Estado de Hidalgo. Unidad Universitaria, carr. Pachuca-Tulancingo, km 4.5. Pachuca, Hidalgo. México. C.P. 42183. Tel. (52) 771- 7172000 ext. 6713. e-mail: franpac@infosel.net.mx

Recibido el 10 de febrero de 2006; aceptado el 15 de enero de 2007

Abstract: In this work, the synthesis, characterization, reactivity in NaOH media and the cyanidation of the ammonium jarosite are approached. The jarosite was synthesized and characterized by several analytical techniques; the granulometric analysis was also performed. The synthesis results show that the material consists of a solid ammonium-hydroniumjarosite-argentojarosite solution of an approximate [$(NH_{4(0.95)}\ Ag_{0.025}\ H_30_{\ 0.025})Fe_{2.66}(SO_4)_2\ (OH)_6$] formula. This jarositic compounds synthesis, along with the mechanical agitation system with seed recycling, has a notable effect on the spheroidization degree and on the particles growth degree, reaching the highest particle sizes of the 44-37μm (> 61%) kind. The decomposition and cyanidation curves show an induction period, a progressive conversion period and a stabilization zone. The SEM-EDS analysis shows an unreacting jarosite core in the progressive conversion period, as well as a gel layer, through which the sulphate ions easily diffuse towards the solution. The alkaline decomposition and the ammonium jarosite cyanidation is a process of two serial stages: A slow alkaline decomposition stage followed by an instant silver complexation stage.

Keywords: Ammonium jarosite, cyanidarion, granulometric analysis, descompositon.

Resumen: En el presente trabajo se aborda la síntesis, caracterización, reactividad en medio NaOH y cianuración de la amoniojarosita argentífera. La jarosita fue sintetizada y caracterizada por diversas técnicas analíticas; también se realizó el análisis granulométrico. Los resultados de la síntesis nos indican que el material consiste de una solución sólida de jarosita de amonio-hidroniojarosita-argentojarosita de fórmula aproximada [$(NH_{4(0.95)}\ Ag_{0.025}\ H_30_{\ 0.025})Fe_{2.66}(SO_4)_2(OH)_6$]. La síntesis de este compuesto jarosítico con el sistema de agitación mecánica y reciclado de semillas tiene un efecto notable en el grado de esferoidización y crecimiento de partículas, alcanzándose con la segunda siembra los mayores porcentajes y tamaños de partícula del orden de 44-37 μm (> 61%). Las curvas de la descomposición y cianuración muestran un período de inducción, un período de conversión progresiva y una zona de estabilización. El análisis por SEM-EDS en la etapa de conversión progresiva muestra un núcleo de jarosita sin reaccionar y una capa de gel a través de la cual los iones sulfato difunden con facilidad hacia la solución. La descomposición alcalina y cianuración de la amoniojarosita es un proceso de dos etapas en serie: una etapa lenta de descomposición alcalina, seguida por una etapa instantánea de complejación de la plata.

Palabras clave: Amoniojarosita, cianuración, análisis granulométrico, descomposición.

Introduction

The jarosite process was developed by the Electrolytic Zinc Company of Australasia, the Zinkkompani (Norway), and by La Real Compañía Asturiana (Spain). It is a double lixiviation process, one acid hot lixiviation, in which a total Zinc ferrite attack is achieved, which leads to high Zinc concentrations with high iron impurities that are precipitated as a jarositic compound at temperatures between 90 and 100°C [1]. The processing of zinc sulphur minerals is the most extensively developed method, and it consists of the following stages: Roasting, leaching and electrowining. Almost 80% of the world's zinc is produced with this process, and the rest is increasingly being produced by electrothermic processes (6%) or by the Imperial Smelting process (12%) [2]. The jarosite precipitation technology is used in the hydrometallurgical circuits of more than 60 zinc plants worldwide, having as main goal the elimination of the Fe, sulphates control, and other impurities, such as Cd, Cu, As, Sb, F, Mn, Ni and Co, in order to improve the filtration stage and the zinc electrolytic process efficiency [3, 4]. Even though these problems are usually solved, another important problem comes out: The incorporation of the silver metallic values to the jarosite structure. Jarosites are placed in the burrows, and that means losses from an economic point of view; with reference to this, a wrong behavior has been observed in the recovery of the contained Ag in those precipitates, via conventional processes [5,6].

In this work, the ammonium jarosite seed recycling is studied in order to improve the morphology and texture and to increase the particles size, having as goal the improvement of the filtering process speed, as well as the study of the reaction nature in NaOH environment and the decomposition products cyanidation of this jarositic compound, in order to establish the best conditions and to recover the silver values contained in those burrows. It is important to mention that we continue to study the ammonium jarosite because it is the most used compound in the electrolytic zinc plants around the world and because the salt (ammonium sulphate) used for its constitution is much cheaper and easy to find in the market.

In Mexico, the jarosite technology is used by Grupo Peñoles (Torreón, Coahuila) and by Industrial Minera México (San Luis Potosí). Each plant produces about 400 tons of jarositic residuals, including 155 g [7,8] of silver per residual ton; if we consider that these electrolytic plants have been working continuously for 30 years, these burrows are obviously attractive from an economic point of view, and that is why we are very interested in this research. The reactivity results of this work are compared to those obtained with other jarositic compounds, such as the argentojarosite [9], natrojarosite [10] and potassium jarosite [11].

Materials and Experimental Procedure

The argentian ammonium jarosite's synthesis was carried out with the methods used by Dutrizac and Kaiman [5]; the conditions were of 0.25M $Fe_2(SO_4)_3 \cdot nH_2O$, 0.3M $(NH_4)_2SO_4$, 0.002M Ag_2SO_4, 2.5g Li_2CO_3 or 1ml H_2SO_4 in 1000 cm^3 of distilled water at 448 s^{-1} or 1200 s^{-1} according to the agitation type; this was performed at 94 ^{0}C for 24 h at a pH of 1.8. The recycling of the seed was performed to increase the particle size of this jarositic compound by applying the technique used by Dutrizac and Jambor [4], Patiño [10] and Dutrizac (12), and it consisted of adding 10 g of the previously obtained jarosite to the solution before reaching synthesis temperature. This technique is successively applied until the fifth sowing is obtained. The magnetic and mechanical agitations were used to evaluate the agitation type effect. For the magnetic agitation, we used a glass kettle of plane bottom mounted on a heating plate, supplied with a magnetic agitation system (with magnetic bar), with a 1200 s^{-1} constant. For the mechanical agitation, we used a glass kettle of round bottom, mounted on a heater or an electric blanket and connected to a 448 s^{-1} double arm stainless steel rotor. Both systems had a fit cooler in order to avoid liquid loss by evaporation.

The jarosite was characterized by chemical analysis, x-ray diffraction (XRD), Sem, x-ray dispersive energy spectrometry (EDS) and granulometric analysis. The DRX (fig. 1) and SEM-EDS (fig. 2) characterizations confirm a monophasic product. In the chemical analysis, the silver was determined by EAA, the iron by titration-dichrometry, the sulphate by gravimetry, the ammonium ion by the Kjeldahl technique and the H_3O and OH ions were estimated by difference; the results are represented in table 1. These compounds density was determined with a picnometer, using water as an immersion environment. The density was 2670 $Kg \cdot cm^3$, which is very similar to the density reported by Dutrizac [5].

By simplicity, these compounds formula was normalized to SO_4=2, OH=6; the alkaline site was normalized to 1 and it is filled with Ag, NH_4 y H_3O; the $H_3O^+ + OH^-$ was calculated by difference. The resulting formula of the synthesized argentian ammonium jarosite is:

$$(NH_{4(0.95)}Ag_{0.025}H_3O_{0.025})Fe_{2.66}(SO_4)_2(OH)_6$$

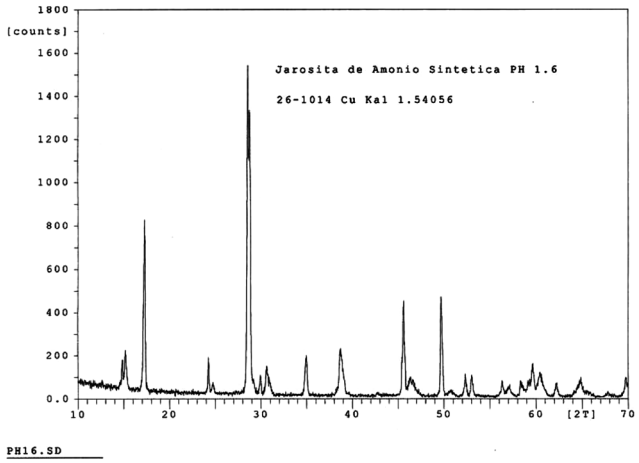

Fig. 1. X-ray diffractogram of the argentian ammonium jarosite.

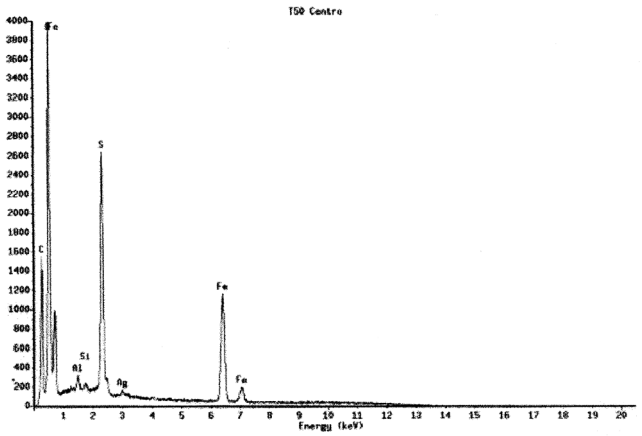

Fig. 2. EDS spectrum of the argentian ammonium jarosite.

Table 1. Chemical composition of the argentian ammonium jarosite.

Element	%
NH_4	3.80
Ag	0.60
Fe	32.48
SO_4	40.40
H_3O^++OH^-	22.72

In table 2, the results of the jarosite synthesis by magnetic agitation with and without sowing are summarized. There we can see that this kind of system does not have a major influence on the particles size growth, measuring much less than 25 μm (>96 %).

In table 3, the granulometric results of the jarosite synthesis by mechanical agitation with and without sowing are presented. In this table, we can notice that this kind of system has a notable effect on the particles size growth, reaching the highest percentages and sizes for the second sowing synthesis. The

Table 2. Magnetic agitation: Granulometric anaylisis of the argentian ammonium jarosite (partial %).

Size (μm)	Without sowing	1st sowing	2nd sowing	3rd sowing	4th sowing	5th sowing
>177	0.08	0.03	0.04	0.03	0.08	0.10
177-149	0.02	-	0.01	0.02	0.01	0.03
149-88	0.07	0.01	0.01	0.05	0.01	0.03
88-74	0.04	0.01	0.01	0.02	0.03	0.04
74-53	0.06	0.01	0.07	0.07	0.33	0.07
53-44	0.02	-	-	0.01	0.03	0.02
44-37	2.07	0.04	0.02	0.03	0.09	0.52
37-25	1.03	0.01	-	-	0.01	0.01
<25	96.61	99.89	99.84	99.77	99.41	99.18

Table 3. Mechanical agitation: Granulometric analysis of the argentian ammonium jarosite (partial %).

Size(μm)	Without sowing	1st sowing	2nd sowing	3rd sowing	4th sowing	5th sowing
>177	0.07	0.06	0.07	0.06	0.05	0.04
177-149	0.02	0.06	0.06	0.05	0.10	0.25
149-88	0.02	0.17	0.17	0.13	0.12	0.20
88-74	0.03	0.29	0.22	0.28	1.35	2.35
74-53	0.24	0.57	4.55	33.02	10.81	13.50
53-44	0.03	0.66	16.45	4.09	3.20	3.61
44-37	6.14	4.71	61.87	4.99	29.83	29.96
37-25	1.24	0.48	2.65	0.12	1.26	0.55
<25	92.21	93.00	13.96	57.26	53.28	49.54

percentages and sizes are much higher than the 44-37 μm family (>61%).

Figure 3 shows a general image picture of the ammonium jarosite that corresponds to the mechanical agitation without sowing. Observe how the sizes distribution matches the results shown in table 3, as a morphology with a strong tendency to sphericity stands out. Figure 4 is a picture of the sifted particles by wet via with the #400 (44-37 μm) Tylor series blanket; this technique allows a good particle size enclosing. Figure 5 is a detailed picture where the particles are built by micro crystals (1-2 μm) which are strongly soldered in a compact texture. These parameters of the synthesized jarosite, purity, sphericity, good enclosing, and compact texture are aspects that, somehow, facilitate the study of the argentian ammonium jarosite chemical reaction topology, as well as afterwards kinetics research of this kind of compounds. For these reasons, the synthesis material used for the study of the ammonium jarosite decomposition and cyanidation corresponds to the 44-37 μm size family, obtained in the second sowing by mechanical agitation.

Experimental procedure

The experimental procedure is based on the research performed by Viñals [6], Roca [9], Patiño [10] and Cruells [11]. The experiments were performed in a 1 L glass kettle which was set on a heating plaque, supplied with a thermostat that allows temperature variations of up to ±0.5 ºC; a magnetic agitation system (magnetic bar), and a pH-meter were used. In order to ensure the ammonium jarosite decomposition process, the following procedure was used: 1) 500 mL of deionized water were poured in the glass kettle and its accessories were

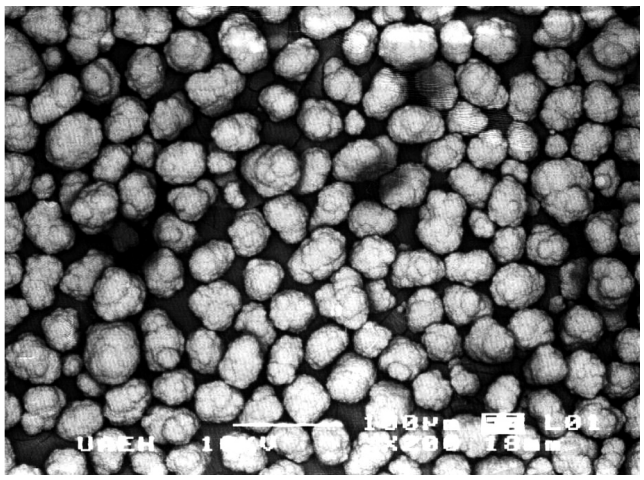

Fig. 3. General particle size view of the argentian ammonium jarosite, synthesized at 94^{0}C-24 h with mechanical agitation, without sowing. SEM.

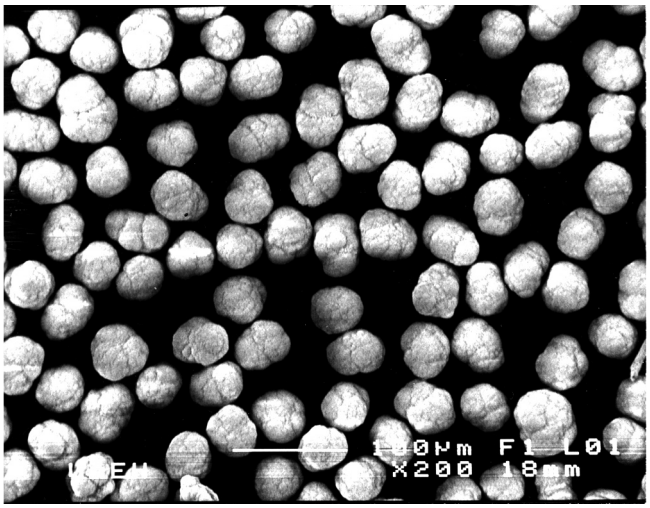

Fig. 4. Image of particle sizes (44-37μm) separated by sifting of the argentian ammonium jarosite, synthesized at 94^{0}C-24h. with double sowing and mechanical agitation. SEM.

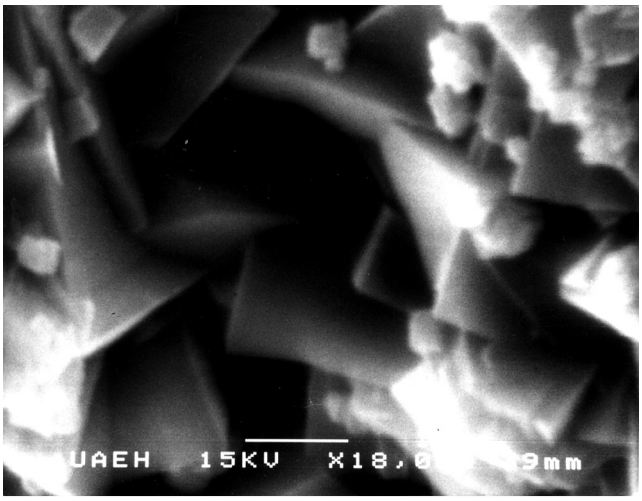

Fig. 5. Detail of a spherical particle of argentian ammonium jarosite with seed sowing, constituted by micro crystals of the rhombohedric kind. SEM.

placed, providing a 1250 rpm agitation. 2) The deionized water temperature was measured, and subsequently, the work temperature was set (30 ºC). 3) NaOH was added until a pH of 11.88 was obtained; the purpose was to obtain a NaOH concentration of 1.1×10^{-2} M. 4) When the pH was adjusted, 0.5 g of jarosite made of enclosed particles of 44-37 μm, were added. The time in which the solids made contact with the liquids was considered as the reaction startup time. 5) Samples of 5ml of the decomposing solution were taken at a determined time and they were filtered and analyzed by ICP (Inductive Coupling Spectrophotometer). The OH^- concentration was calculated considering the water ionic product constant [13] and the alkaline solution pH in accordance with the work temperature we used here. Since the alkaline decomposition stechiometry research shows that the elimination of the lattice sulphate ions and their fast diffusion towards the solution are produced, the decomposition procedure was performed through the sulphate ions analysis via ICP. The decomposed jarosite fraction x was estimated with $x = k_t/k_f$, where k_t is the sulphur concentration at a specific time t, and k_f is the sulphur concentration when the jarosite has reached total decomposition.

As to the cyanidation, we employed a similar procedure to the one used for the decomposition; however, and atomic absorption spectrometer was used this time. The cyanidation follow-up was performed by analyzing the silver. The cyanidated silver fraction was calculated with $x = Ag_t/Ag_f$, where Ag_t is the silver concentration at a specific time t, and Ag_f is the silver concentration when the jarosite has reached total cyanidation. As a follow-up alternative method of the argentian jarosite decomposition, a resulting liquid study was performed via gravimetry, setting the sulphate amount at different times. The following procedure was carried out: The reactor and its accessories were assembled on the heating module; 1000 ml of deioinized water were added; the pH was measured at room temperature and at 30ºC; later, NaOH was added until a 1.1×10^{-2} M NaOH solution concentration and a pH of 11.88 were obtained. Immediately, 1gr. of ammonium jarosite, with enclosed particle sizes of 44-37μm was added at an agitation speed of 1250 rpm in order to maintain the solids in suspension, and to avoid the diffusion effect on the liquid film. At different and prefixed times, the decomposition reaction was neutralized with HCl (at 2%). The reactor was disassembled and the resulting solution was filtrated in vacuum. The solids were washed and the obtained solution was evaporated until 10ml were obtained and subsequently analyzed by gravimetry. The decomposed fraction was calculated with $x = k_t/k_f$, where k_t is the sulphur concentration at a specific time t. and k_f is the sulphur concentration when the jarosite has reached total decomposition.

The resulting solids at different decomposition and cyanidation times were exhaustively characterized by chemical means, by x ray diffraction and by scanning electron microscopy, combined with x ray dispersive microanalysis.

Results and discussion

The ammonium jarosite synthesis.

The synthesis product obtained under the above-mentioned conditions consists of a solid solution with an approximate $[(NH_{4(0.95)}Ag_{0.025}H_3O_{0.025})Fe_3(SO_4)_2(OH)_6]$ formula, whose results, obtained by DRX (Fig.1) and EDS (Fig. 2), prove that it corresponds to the ammonium jarosite. They also correspond to the results obtained by Dutrizac [5] under similar conditions. The ammonium jarosite synthesis leads to a spheroidal-type particle formation; these particles are constituted by rombohedric crystals which are strongly interconnected in a compact texture. Observe how the mechanical agitation has a strong effect on the particle size growth. The consecutive sow-

Table 4. SO_4^{2-} and Ag^+ extraction at different decomposition and cyanidation times of the argentian ammonium jarosite; 37 to 44 μm, NaOH 1.1 × 10^{-2}M, NaCN 2.55 × 10^{-3}M, pH 11.88 and 30ºC.

	Gravimetry SO_4^{-2}		ICP P las ma S		Atomic absorption EEA Ag^+	
time (min)	extraction percentage	$1-(1-x)^{1/3}$	extraction percentage	$1-(1-x)^{1/3}$	extraction percentage	$1-(1-x)^{1/3}$
0	0	0	0	0	0	0
5	3.31	0.01	3.49	0.01	-	-
10	5.51	0.02	9.77	0.03	-	-
15	12.70	0.04	20.62	0.07	-	-
16	-	-	-	-	11.86	0.04
20	22.1	0.08	34.55	0.13	19.05	0.07
24	-	-	-	-	29.40	0.11
28	-	-	-	-	42.08	0.17
30	43.09	0.17	57.29	0.25	-	-
32	-	-	-	-	55.80	0.24
36	-	-	-	-	69.07	0.32
40	58.29	0.25	77.77	0.39	78.50	0.40
44	-	-	-	-	84.29	0.46
48	-	-	-	-	89.00	0.52
50	68.50	0.32	82.92	0.44	-	-
52	-	-	-	-	93.87	0.61
60	77.64	0.39	90.24	0.54	98.22	-
80	94.75	0.62	100.00	1.00	100.00	-
100	98.62	0.76	100.00	1.00	100.00	-
120	100.00	1.00	100.00	1.00	100.00	-

ings allow the additional increase of the jarositic compounds particle size growth.

The results of our work, which consists of two consecutive synthesis of argentian ammonium jarosite with particle sowing, are consistent with the results obtained for the silver jarosite (14), argentian sodium jarosite (10) and the argentian potasium jarosite (11), obtaining spheroidal particles that reach 150 μm and which are made of rombohedric crystals of 0.5-1.5 μm; however, these results are remarkably different from the results obtained with the argentian plumbojarosite(14), where irregular and incoherent aggregates (1-10 μm) (with a grape cluster-like morphology), constituted by rombohedrical micro crystals (0.5-1.5 μm) are formed. This difference can be attributed to the fact that the precipitation reaction of the NH_4^+, Ag^+, Na^+ y K^+ jarosites occurs in a homogenous media, while the precipitation reaction of the argentian plumbojarosite occurs in a heterogeneous media due to the low solubility of the $PbSO_{4(s)}$,which explains the difference of the growth among the jarosite-type compounds. It is important to mention that Dutrizac [12] contributed to the study of the effect of the seed sowing on the growth of sodium jarosite particles. But he did not study the effect of the sowing on the growth of the particle sizes of the ammonium jarosite. For this reason, our synthesis method with seed recycling is a contribution that allows the establishing of the best sowing conditions to reach the highest particle sizes and percentages.

Table 4 shows the obtained data for the argentian ammonium jarosite decomposition and cyanidation by sulphate (via gravimetry and ICP) and silver determination (EAA), respectively. Figure 6 graphically represents the obtained results. As this "s" type figure shows, the alkaline decomposition presents an induction period, in which the jarosite external aspect (yellow colored) remains with no alteration, which can be seen on table 4, where the sulphate ion concentration is found at insignificant levels. This makes us think that the induction period is a superficial phenomenon at a molecular thickness level, which is related to absorption processes, whose mechanism needs to be studied with other techniques that are not approached here. However, the induction period is presumed to be the result of the OH ions chemical absorption on the cationic superficial centers, which in principle would appear inaccessible due to the coordination of the sulphate and OH ions of the jarosite lattice. By all means, this induction time is an active point creation period until the reaction front is established. The induction period can be eliminated, whether by chemical or mechanical methods, but it was not eliminated in this work because in this way we could generalize this behavior with the behavior of other jarosites. The end of the induction period is recognized by a change in the superficial color of the solid, which changes from yellow to a reddish color. Simultaneously, the sulphate level in the solution increases progressively until a stabilization period is reached; this indi-

cates that the reaction has ended. Observe how, in figure 6, the cyanidation curve is similar to the ones obtained by decomposition; this leads us to assure that the decomposition and cyanidation speeds are similar; therefore, the cyanide has no effect on the decomposition, and an instant stage of the decomposition product complexation occurs until 100% silver extractions are reached.

Reaction topology

The data in figure 6 and in table 4 are treated with the model of spheroidal particles of decreasing nuclei, where the chemical reaction is the stage that controls the global process.

$$1-(1-x)^{1/3} = k_{exp}t \qquad (1)$$

Where k_{exp} is the experimental constant of the reaction speed, t is the time at a determined reaction degree and x is the decomposed particle fraction at a time t. Observe how, in figure 7, the experimental data of the alkaline decomposition and cyanidation adapt themselves to the model defined in equation 1. The spectrum of figure 8, obtained by DRX, shows the decomposed ammonium jarosite solids and it also shows how the decomposition reaction progressively increases with time, which can be confirmed in the argentian ammonium jarosite reticular plans, which become progressively weak until they totally disappear in long reaction periods; this gives as a final result, an amorphous compound that does not evolve to crystal stages in the conditions we studied.

The scanning electron microscopy test and EDS of a smoothed section of a partially decomposed solid particle reveal the presence of a reaction front, as it is shown in figure 9. Here we can see that there is an unreacting jarosite nuclei and a hydroxide gel halo through which the sulphate ions easily diffuse.

Figures 2 and 10 correspond to the EDS-obtained microanalysis that matches the SEM-obtained image for a partially decomposed jarosite. The unreacting jarosite nuclei spectrum indicates that the jarosite chemical composition in this area remains unalterable. The decomposed areas spectrum reveals the elimination of the sulphate ions in the jarosite lattice towards the solution; this leads us to state that the decomposed area is made of a hydroxide gel that allows the sulphate ions to diffuse towards the solution. For this reason, we state that the solution's OH ions diffuse easily through the jarosite lattice, settling a reaction front in which the diffusion process occurs.

According to the above, the stechiometry of the decomposition process in NaOH environment can be expressed with the following reaction:

$$NH_4Fe_3(SO_4)_2(OH)_{6(s)} + 3OH^- \rightarrow NH^+_{4(aq)} + 3Fe(OH)_{3(s)} + 2SO^{-2}_{4(aq)} \qquad (2)$$

Since the experimental data of the silver extraction by means of alkaline cyanidation easily fit the ammonium

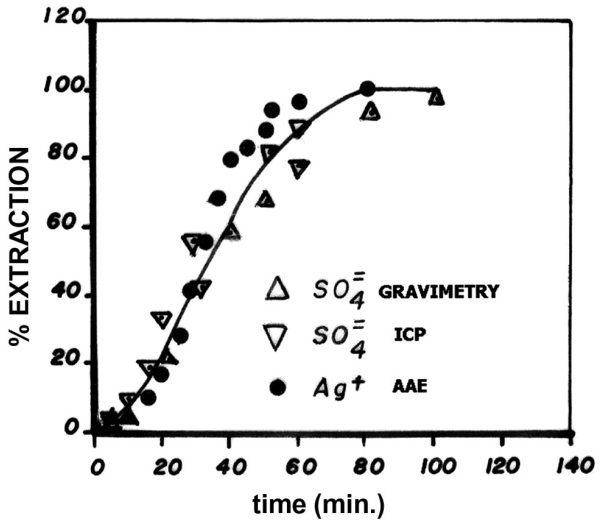

Fig. 6. Alkaline decomposition and cyanidation curves of the argentian ammonium jarosite, ph 11.88, 30 °C and 37 μm.

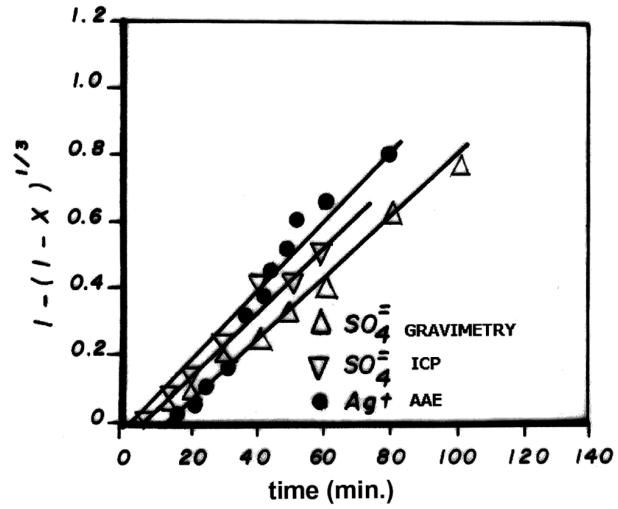

Fig. 7. Representation of the decreasing nuclei and chemical control for the data in figure 6.

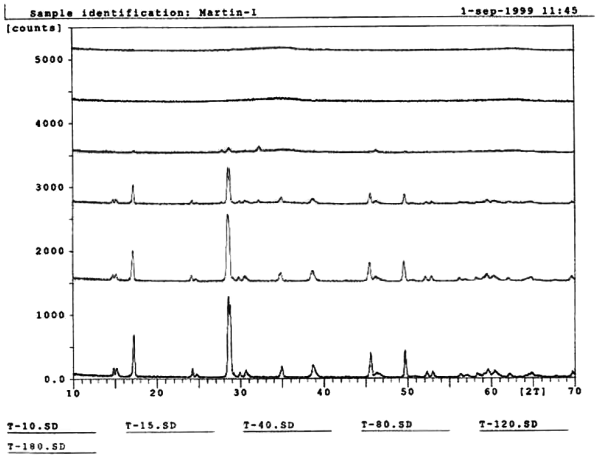

Fig. 8. Spectrum obtained by DRX for different decomposition times of the argentian ammonium jarosite, ph 11.88, 30 °C, 37 μm.

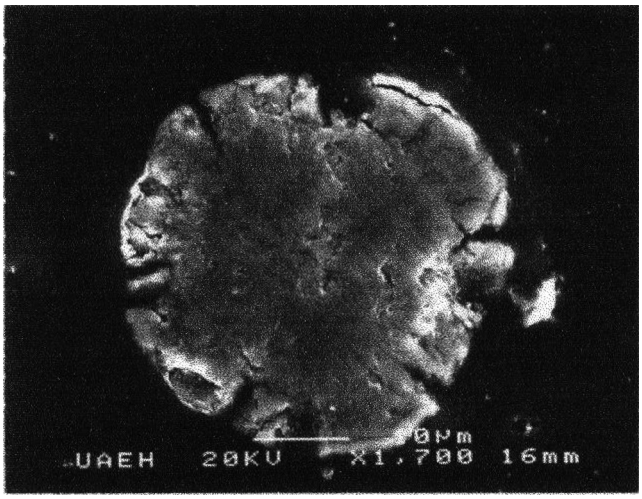

Fig. 9. Image of an argentian ammonium jarosite's particle (37-44), partially decomposed with NaOH, pH 11.88, 50 min., 30 °C. SEM.

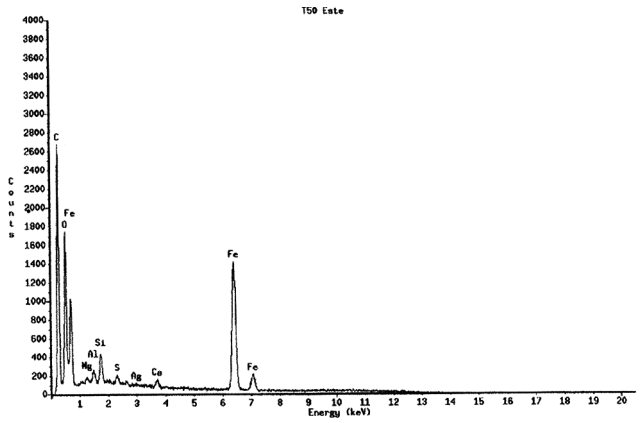

Fig. 10. EDS spectrum that corresponds to the argentian ammonium jarosite's decomposition in NaOH environment, periphery, 50 min.

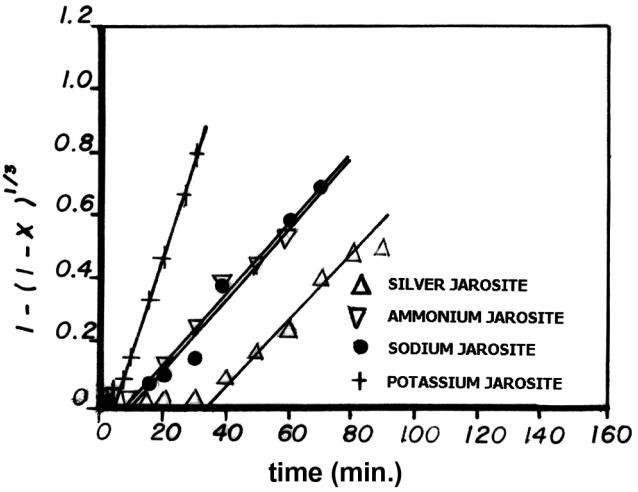

Fig. 11. Representation of the decreasing nuclei and chemical control of the silver, ammonium, sodium and potassium jarosite for the data in figure 7.

Table 5. Value of the $1–(1–x)^{1/3}$ term depending on the decomposition time of the silver, ammonium, sodium and potassium jarosite, respectively; 37-44 μm, NaOH 1.1×10^{-2} and 30 °C.

	$1 - (1 – x)^{1/3}$			
Time (min)	Silver Jarosite	Ammonium Jarosite	Sodium Jarosite	Potassium Jarosite
2	-	-	0.020	-
3	-	-	-	0.070
5	-	0.012	0.012	0.020
7.5	-	-	-	0.092
10	-	0.034	-	0.154
15	0.004	0.074	0.070	0.330
20	0.008	0.132	0.110	0.470
25	-	-	0.149	0.667
30	0.023	0.247	0.183	0.779
40	0.082	0.394	-	-
45	-	-	0.381	-
50	0.166	0.445	-	-
60	0.238	0.540	0.590	-
70	0.399	-	0.703	-
80	0.476	-	-	-
90	0.491	-	-	-

jarosite decomposition curve, they also fit the chemical control model. This indicates that the alkaline decomposition speed does not depend on the NaCN effect, therefore, the ammonium jarosite cyanidation can be described through two serial stages: A slow decomposition stage, defined by equation 2 that controls the global process, followed by an instant complexation stage of the reaction products:

$$Ag(OH)_{(s)}+2CN^-_{2(aq)} \rightarrow 2Ag(CN)^-_{2(aq)}+(OH)^-_{(aq)} \qquad (3)$$

The obtained results via chemical analysis, x ray diffraction, scanning electron microscopy, and x-ray dispersive energy spectrometry confirm that the alkaline decomposition and cyanidation stechiometry of the argentian ammonium jarosite in NaOH environment can be represented by equations 2 and 3.

Comparison of the $1–(1–x)^{1/3}$ term for the silver, ammonium, sodium and potassium jarosite decomposition, respectively. Figure 11 is obtained from the data shown in table 5, which is a comparative representation of the decreasing nuclei and of the chemical control of different argentian jarosites. There we can see how the argentian silver, ammonium, and sodium jarosites have almost the same slope or speed experimental constant, respectively; however, the argentian potassium jarosite has a greater speed experimental constant than those of the other jarosites studied so far. This constant is related to the substitution level of Ag, NH_4, Na, K and H_3O in the crystal structure of the jarosites [15].

Conclusions

The argentian ammonium jarosite synthesis in conditions of 0.25 M $Fe_2(SO_4)_3 \cdot n\ H_2O$, 0.3 M $(NH_4)_2SO_4$, 0.002 M Ag_2SO_4, 94ºC, 24 h, 448 rpm, leads to the obtaining of a solid solution of ammoniumjarosite-hydroniumjarosite-argentojarosite of approximate formula:

$$(NH_{4(0.95)}Ag_{0.025}H_3O_{0.025})Fe_{2.66}(SO_4)_2(OH)_6$$

whose morphology consists of spheroidal particles made of rombohedrical crystals strongly soldered in a compact texture.

The ammonium jarosite synthesis with seed recycling and mechanical agitation has a strong effect on the particle size growth, observing that in the second sowing the highest percentages with the highest particle size (37-44μm) are obtained. This size family has been used to perform the topology study of the argentian ammonium jarosite reaction.

The alkaline decomposition and alkaline cyanidation curves of the argentian ammonium jarosite show and induction period, followed by a progressive conversion period, until the stabilization zone is reached.

During the induction period, no superficial or composition changes are observed in the jarositic phase.

The progressive conversion period appears after the reaction front is established, and an iron hydroxide gel halo is formed on an unreacting jarosite nuclei. This gel allows an easy diffusion of the SO_4^{-2} and Ag^+ reaction ions towards the watery phase.

The ICP method via sulphur and the gravimetry via sulphates, both derived from the alkaline decomposition, or the atomic absorption for cyanidation-extracted silver can be used to follow the argentian ammonium jarosite reaction topology.

The alkaline decomposition of the ammonium jarosite in NaOH environment can be represented according to the following stechiometry:

$$NH_4Fe_3(SO_4)_2(OH)_{6(s)} + 3OH^- \rightarrow NH_{4\ (aq)}^{+} + 3FeOH_{3(s)} + 2SO_{4\ (aq)}^{-2} \quad (2)$$

The experimental data in the progressive conversion stage fit the model of the constant size spheroidal particle with decreasing nuclei and chemical control, whose kinetics equation is:

$$k_{exp}t = 1-(1-x)^{1/3} \quad (1)$$

The comparison of the k_{exp} of the speeds of the reaction process under the studied experimental conditions allows us to state that the ammonium jarosite's cyanidation can be described in 2 series stages: A decomposing stage which controls the global process (equation 2), followed by an instant complexation stage of the decomposition products. The following equation defines it:

$$Ag(OH)_{(s)} + 2CN^-_{2(aq)} \rightarrow 2Ag(CN)^-_{2(\ aq)} + (OH)^-_{(aq)} \quad (3)$$

Acknowledgments.

We thank CONACyT for sponsoring this work, the Metallurgy and Materials Investigation Center at the UAEH, for their support and for letting use their research facilities, and the Serveis Científicotècnicos of the Universitat de Barcelona for their valuable help in the completion of this work.

References

1. Limpo, J. L.; Siguin, D.; Hernández, A. *Metalurgia* CENIM **1976**, *12*, 81-87.
2. Pelino, M.; Cantalini, C. *Hydrometallurgy*, **1996**, *40*, 25-37.
3. Dutrizac, J. E. *Metall. Mater Trans. B*, **1993**, 531-539.
4. Dutrizac, J. E.; Jambor, J. L. *Appl. Mineral.* Park, W. C.; Hausen, D. M;. Hagni, R. D. eds., AIME Warrendale, **1984**, 507-530.
5. Dutrizac, J. E.; Kaiman, S. *Can. Mineral.*, **1976**, *14*, 151-158.
6. Viñals, J.; Núñez, C. *Metall. Mater Trans. B*, 1988, *19B*, 365-373.
7. Salinas, E. Caracterización y Cinética de la Descomposición Alcalina y Cianuración de Amoniojarosita Generada en Circuitos Hidrometalúrgicos de Zinc. Tesis de Doctorado, Universidad de Barcelona, 1998.
8. Plata, M. Cinéticas de Descomposición y Cianuración de Amoniojarosita-Argentífera en Medio NaOH. Tesis de Licenciatura, Universidad Autónoma del Estado de Hidalgo, **2001**.
9. Roca, A.; Patiño, F.; Viñals, J. *Hydrometallurgy* **1993**, *33*, 341-358.
10. Patiño, F.; Salinas, E.; Cruells, M.; Roca, A. *Hydrometallurgy* **1998**, *49*, 323-336.
11. Cruells, M.; Roca, A.; Patiño, F.; Salinas, E.; Rivera, I: *Hydrometallurgy* **2000**, *55*, 153-163.
12. Dutrizac, J. E. *Hydrometallurgy* **1996**, *42*, 293-312.
13. *Handbook of Chemistry and Physics*; CRC Press, 12th Ed., **1991-1992**, 8-42.
14. Patiño, F. *Rev. Soc. Quím. Méx.* **1993**, *37*, 51-62.
15. Roca, A.; Cruells, M.; Patiño, F.; Rivera, I.; Plata, M. *Hydrometallurgy* **2006**, *81*, 15-23.